

Modelling of the Hydrogen Diffusion in Martensitic Steel in contact with H₂SO₄ Media

J. Bouhattate*¹, S. Frappart^{1,2}, and X. Feaugas¹

¹*Laboratoire d'études des matériaux en milieux agressifs (LEMMA)

Université de La Rochelle, Bat. Marie Curie, av. Michel Crépeau 17042 La Rochelle

² V&M France – CEV, 60 route de Leval, F-59620 Aulnoye-Aymeries, France

jamaa.bouhattate@univ-lr.fr

Abstract: Hydrogen Embrittlement (HE) is one of the mechanisms responsible for premature failure of structures (petroleum industries, pipelines, water conduit...). In the context of environmental sustainability, it is compelling to improve or conceive new processes and/or new materials capable of reducing fracture induced by HE. The purpose of this article is to analyze the influence of the oxide layer on the permeability of hydrogen. This investigation was carried on as a correlative effort with experimental tests completed on a steel with a quenched and tempered martensitic microstructure within acid media (H₂SO₄).

In this project finite element modeling using Comsol Multiphysics software is needed to get abounding data concerning the apparent diffusion coefficient. Hydrogen concentration, variation of the thickness and the diffusion coefficient of the oxide layer may affect the apparent diffusion coefficient. Phenomenological laws have been derived to approach true diffusion coefficient and average hydrogen concentration as a function of apparent diffusion coefficient and hydrogen concentration at the entry side of the sample.

Keywords: Hydrogen embrittlement (HE), Diffusion, Permeation tests, Oxide layer, Corrosion.

1. Introduction

Because of its particular structure, hydrogen is part of many fundamental research investigations in physics and chemistry. It is also highly inspected in industrial research because of the hydrogen embrittlement that occurs frequently in industrial environments. Studies about hydrogen diffusion in steels are often implemented using permeation tests. It was first developed [1] to examine hydrogen diffusion within palladium, and is today employed for many metals (nickel, steels...). Permeation tests

allow to easily measure the hydrogen flux through a metallic membrane and so are relevant apparatus to characterize the hydrogen-metal interactions. It can also reveal surface phenomena such as corrosion or impact of an oxide film. The obtained curves can provide quantitative information: the apparent diffusion coefficient, the subsurface concentration C_0 and the steady-state permeation rate. However to access the true diffusion coefficient and the average concentration, hard hypothesis are generally imposed to interpret experimental data. More specifically, the surface state and the oxide layer haven't been taken into account.

In order to increase our knowledge of the interactions of hydrogen with steels, the purpose of this research is to simulate the diffusion of hydrogen through quenched and tempered high strength low alloys (HSLA) with oxide layer by using finite element methods (FEM).

2. Permeation tests

The permeation test is realized through a metallic membrane and is composed of a cell divided in two sections: a charging cell (source of hydrogen) and a detection cell (diffused hydrogen oxidation and creation of a proportional current) divided by a metallic membrane (the sample). Figure 1 represents the principle of hydrogen electrochemical permeation test. The electrochemical reactions characteristics are the electrochemical adsorption and the reduction of the proton in the charging cell in acid media:



A part of the hydrogen is then absorbed and diffused through the steel membrane. On the detection side, the anodic polarisation oxidizes the diffused hydrogen:



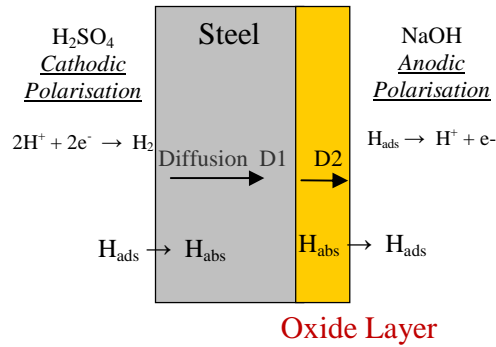


Figure 1. Principle of hydrogen electrochemical permeation test

The charging solution can be acid, such as sulfuric acid H_2SO_4 0.5M [2-4], H_2SO_4 0.1M [5,6] or an alkaline solution such as NaOH 0.1M [3-9]. The usual detection solution is NaOH 0.1M [1,3,5,11,12]. However, the exit polarization might not be a sufficient condition to oxidize all the diffused hydrogen [13].

In fact a passive layer could decrease the oxidation rate which leads to an increase in hydrogen concentration at the exit surface. If the level of hydrogen is high enough, it could induce the hydrogen recombination ($\text{H}_{\text{ads}} + \text{H}_{\text{ads}} \rightarrow \text{H}_2$).

Consequently, some information might be lost since the non oxidized atoms are not accounted in the permeation current. Some authors [5, 13] coated the sample with a palladium layer to ensure the oxidization of all the hydrogen and to avoid the molecular recombination.

3. Diffusion laws

In the classical permeation technique by Devanathan and Stachursky [1, 14], a thin metal membrane of thickness e is placed between two independent electrochemical cells. Hydrogen is introduced on the entry side ($x=0$), diffuses through the membrane and is immediately oxidized on the exit side ($x=e$).

The convenience of permeation techniques is based on the presumption that the conditions of diffusion are established beneath the entry side, where the concentration of hydrogen C_0 is supposed to be constant.

The main problem consists in the presence of a passive layer on the exit side. The stability of the oxide layer may control the diffusion phenomenon and can have consequences on the experimental results. That is to say that diffusion curves correspond to a multilayered system with two different materials and their own diffusion coefficient D (D_1 for the steel and D_2 for the oxide layer).

Thus, only an apparent diffusion coefficient D_{app} can be determined, if we consider the system (steel + oxide layer) as a homogeneous representative volume element (HRVE).

Fick's laws (3) (4) describe diffusion into the multilayered system assuming that there is no hydrogen trapping and the diffusion is unidirectional:

$$J(x,t) = -D_{\text{app}} \frac{\partial C(x,t)}{\partial x} \quad (3)$$

$$\frac{\partial C}{\partial t} = D_{\text{app}} \frac{\partial^2 C}{\partial x^2} \quad (4)$$

Two analytical solutions of Fick's laws are employed to fit the diffusion phenomenon when the hydrogen concentration is supposed to be constant beneath the entry side $C=C_0$ and equals to zero on the exit side $C=0$:

$$J_t = J_{\infty} \frac{2}{\sqrt{\pi\tau}} \exp\left[\frac{-1}{4\tau}\right] \text{ for } \tau = \frac{D_{\text{app}}t}{e^2} \leq 0.3 \quad (5)$$

$$J_t = J_{\infty} (1 - \exp(-\pi^2\tau)) \text{ for } \tau = \frac{D_{\text{app}}t}{e^2} \geq 0.2 \quad (6)$$

Where J_t is the measured permeation rate at time, J_{∞} is the steady-state permeation rate, t is the time (s), e is the thickness of the membrane (m) and D_{app} is the apparent diffusion coefficient (m^2/s)

4. Numerical Model

In order to determine the repercussion of the oxide layer on the hydrogen diffusion and on the apparent diffusion coefficient D_{app} , we simulated our model with the diffusion module of COMSOL Multiphysics.

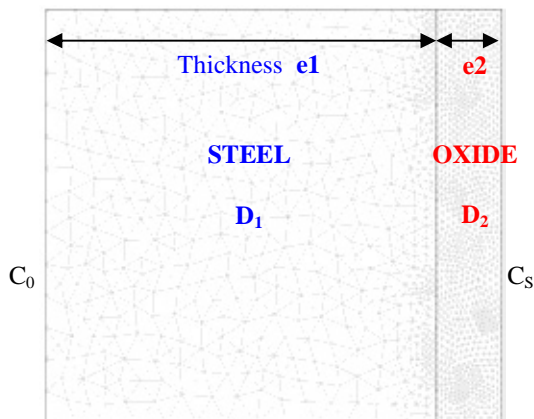


Figure 2. Geometrical data of the problem and 2D meshing

The studied model is described in figure 2. The boundary conditions are $C_0=5 \text{ mol/m}^3$, $C_S=0 \text{ mol/m}^3$. We considered ferritic and martensitic steels since these two metals have a very different diffusion coefficient. Ferritic steels are our model of comparison and $D_1=1.10^{-8} \text{ m}^2/\text{s}$ whereas for martensitic steels, $D_1=7.10^{-10} \text{ m}^2/\text{s}$. For both cases, we modified the oxide layer properties D_2 as follow: $D_2= R.D_1$ with $R \in [10^{-4}-1]$. Doing so enabled us to determine the effects of the oxide layer on the apparent diffusion coefficient D_{app} . The steel thickness is of 1 mm and the oxide layer thicknesses were of 100 nm, and 500 nm.

5. Results

The evolution of the flux at the exit side as a function of R for both thicknesses (100nm and 500 nm) of the oxide layer is plotted in figure 3. We can easily notice the decrease of the flux as R diminishes, and it is much more visible for the thicker layer.

From figure 4, we can observe that the evolution of the apparent diffusion coefficient does not depend on the substrate, but on the characteristics of the oxide layer. Up to $R=0.01$, the variation of D_{app} is insignificant and would correspond to the “real” diffusion coefficient of the substrate (D_1).

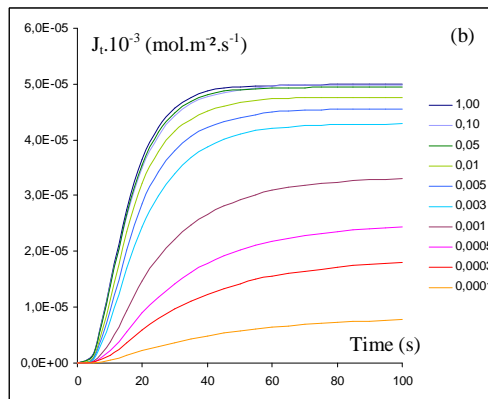
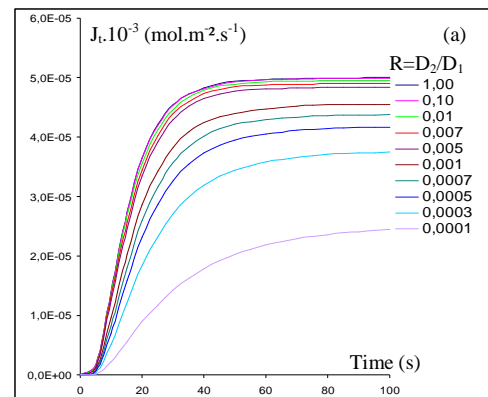


Figure 3. Evolution of the permeation curves in function of R for (a) $e_2=100\text{nm}$ and (b) $e_2=500\text{nm}$

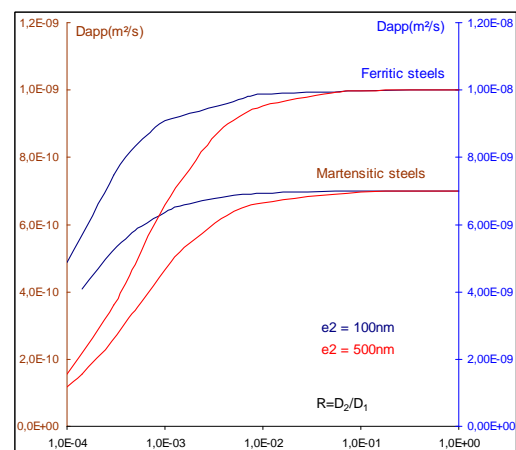


Figure 4. Evolution of D_{app} in function of R

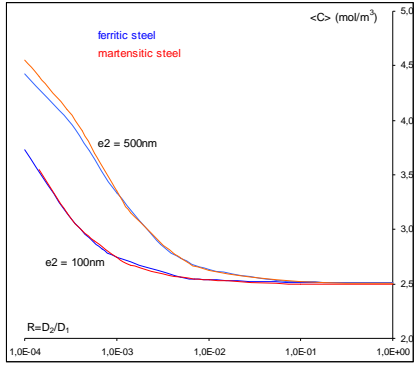


Figure 5. Evolution of $\langle C \rangle$ in function of R and the microstructure of the steel

Figure 5 shows that the average hydrogen concentration in the steel, $\langle C \rangle$, depends only on R and the thickness of the oxide layer. It verifies the hypothesis that the apparent diffusion coefficient, the hydrogen concentration $\langle C \rangle$ and the steady-state permeation rate are mainly determined by the oxide layer on the exit side of the permeation cell.

6. Discussion

It seems that until $R=0.01$ there is no significant variation in D_{app} and $\langle C \rangle$ even with a variation of thickness. In our simulations, the smallest thickness prospected was 100nm whereas in literature [15], the oxide layer could be as thin as 2.8nm. Simulation for such gradient of measure (substrate of 1mm to a layer of 3nm) would demand extensive calculations.

By fitting the obtained curves ($\langle C \rangle$ vs R , D_{app} vs R), we were able to acquire their expression:

$$D = D_{app} \left[1 - \exp \left[- \left(\frac{R}{B} \right)^n \right] \right]^{-1} \quad (7)$$

where $B = B_0 e + B_1$ and n a constant

$$\langle C \rangle = \frac{C_0}{2} \left[1 + \exp \left[- \left(\frac{R}{B} \right)^n \right] \right] \quad (8)$$

From the fitted curves, we can assume that the smaller the oxide layer the bigger the difference between D_1 (substrate) and D_2 (oxide) can be without altering neither D_{app} nor $\langle C \rangle$.

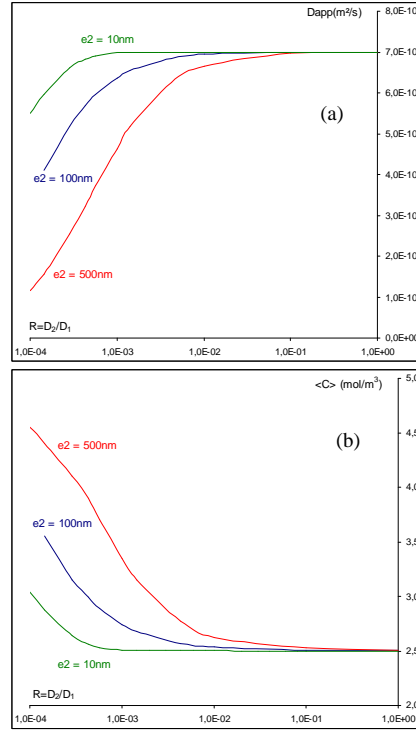


Figure 6. Evolution of fitted of D_{app} (a) and $\langle C \rangle$ (b) in function of R for a martensitic steel for $e_2=10\text{nm}$

Equations (7) and (8) confer an easy evaluation of $\langle C \rangle$ and true D with experimental data if we know the oxide thickness and the oxide diffusion coefficient.

7. Conclusions

This analysis was carried out in order to exhibit the relationship between the oxide layer characteristics and the hydrogen diffusion in HSLA steels in contact with acid media in the charging cell. To do so, we simulated our model using the diffusion module of COMSOL Multiphysics. We were able to obtain interesting results showing that D_{app} and $\langle C \rangle$ rely on the thickness and the diffusion coefficient of the oxide layer. However the thinner is the layer, the smaller is the error committed on the diffusion coefficient of the substrate. FEM calculation offers the opportunity to correct experimental data and the evolution of true diffusion coefficient.

8. References

1. M.A.V. Devanathan, Z. Stachursky, The adsorption and diffusion of electrolytic hydrogen in palladium, *The Royal Society*, **Vol.270**, pp 90-102 (1962)
2. J. Yao, J.R. Cahoon, Experimental studies of grain boundary diffusion of hydrogen in metals, *Acta Met. And Mat.*, **Vol. 39**, No 1, pp 119-126 (1991)
3. N. Parvathavarthini, S. Saroja, R.K. Dayal, Influence of microstructure on hydrogen permeability of 9%Cr-1%Mo ferritic steel, *J. Nucl. Mat.*, **Vol. 264**, pp 35-47 (1999)
4. A.M. Brass, J. Chene, Influence of hydrogen transport and trapping in ferritic steels with electrochemical permeation technic, *Env. Induced Crac. Of Mat.*, pp215-225 (2008)
5. M. Jerome, Interactions Hydrogène-Métal et permeation électrochimique, *Mémoire d'HDR*, Université de technologie de Compiègne (2003) French
6. C. Ly, Caractérisation d'aciers à très haute limite d'élasticité vis-à-vis de la fragilisation par l'hydrogène, *Thèse de Doctorat*, Ecole Centrale Paris (2009)
7. M. Garet, A.M. Brass, C. Haut, F. Gutierrez-Solana, Hydrogen trapping on non metallic inclusions in Cr-Mo low alloy steels, *Corrosion Science*, **Vol.40**, N°7, pp 1073-1086 (1998)
8. Y.F. Cheng, Analysis of electrochemical hydrogen permeation through X-65 pipeline steel and its implications on pipeline stress corrosion cracking, *International Journal of Hydrogen Energy*, **Vol.32**, pp 1269-1276 (2006)
9. V.P. Ramunni, T. De Paiva Coelho, P.E.V. de Miranda, Interaction of hydrogen with the microstructure of low-carbon steel, *Materials Science and Engineering A*, **435-436**, pp 504-514 (2006)
10. A.M. Brass, A. Chanfreau, Accelerated diffusion of hydrogen along grain boundaries in nickel, *Acta Materialia*, **Vol.44**, N° 9, pp 3823-3831, (1996)
11. K. Banerjee, U.K. Chatterjee, Hydrogen permeation and hydrogen content under cathodic charging in HSLA 80 and HSLA 100 steels, *Scripta Materialia*, **Vol.44**, pp 213-216, (2001)
12. L.W. Tsay, W.C. Lee, W.C. Luu, J.K. Wu, Effect of hydrogen environment on the notched tensile properties of T-250 maraging steel annealed by laser treatment, *Corrosion Science*, **Vol.44**, pp 1311-1327 (2002)
13. P. Manolatos, M. Jerome, J. Galland, Necessity of a palladium coating to ensure hydrogen oxidation during electrochemical permeation measurements on iron, *Electrochimica Acta*, **Vol.40**, N°7, pp 867-871 (1995)
14. M.A.V Devanathan, Z. Stachursky, The mechanism of hydrogen evolution on iron in acid solutions by determination of permeation rates, *Journal of the electrochemistry society*, **Vol.111**, N°5, pp 619-623 (1964)
15. T. Casanova, J. Crousier, The influence of an oxide layer on the hydrogen permeation through steel, *Corrosion Science*, **Vol.38**, N°9, pp 1535-1544 (1996)